JOURNAL OF THE ELECTROCHEMICAL SOCIETY

SOLID-STATE SCIENCE AND TECHNOLOGY

MARCH 1974

Oscillatory Interface Instability During Czochralski Growth of Heavily Doped Germanium

R. Singh,*,[1] A. F. Witt,** and H. C. Gatos**

Department of Metallurgy and Materials Science, Massachusetts Institute of Technology, Cambridge, Massachusetts 02139

ABSTRACT

Oscillatory interface instability associated with constitutional supercooling was established during growth of germanium single crystals from gallium-doped melts by the Czochralski technique. The wavelength and phase velocity of the instability were determined and found to be consistent with theory. The effects of pulling and rotation rates on oscillatory instability were quantitatively correlated with the interface stability theory. It was shown that during rotational pulling under conditions leading to constitutional supercooling, the destabilizing effects of rotation dominate its stabilizing effects for moderate rates of rotation in the presence of thermal asymmetry.

During crystal pulling from a doped melt, the region ahead of the growth interface may become constitutionally supercooled if the distribution coefficient of the solute differs from one. The original criterion for constitutional supercooling of Rutter and Chalmers (1) and Tiller *et al.* (2) was derived from static considerations. Constitutional supercooling during crystal growth from stirred melts was first investigated by Hurle (3). Dynamic theories for small perturbations were subsequently developed in the linear approximation by Mullins and Sekerka (4) and by Voronkov (5). Calculations of the conditions leading to instability of solid-liquid interfaces have recently received considerable attention (6-13). In these investigations the melt was considered to be stationary with diffusion being the only means of mass transport; convection effects were excluded. Hurle (13) considered the effects of convective mixing of solute in the melt (expressed in terms of boundary layer thickness) and concluded that the spatial frequency of the first appearing instability is a function of convective mixing. Delves (14, 15), in a recent analysis of interface stability during growth from stirred melts, has predicted oscillatory behavior of the growth interface for convection controlled solute transport encountered in Czochralski growth. Some experimental results consistent with this theoretical treatment have been reported (16).

In the present paper a detailed analysis of an experimental investigation on interface instability during Czochralski growth is reported and discussed in the light of the prevailing theoretical models.

Experimental Procedure

Single crystals of germanium were grown in the <111> direction by the Czochralski technique from gallium-doped melts. The pulling rate, the rotation rate, and the dopant concentration in the melt were adjusted so that the growth interface came to the verge of instability at some point during growth. The diameter of the crystals was maintained between 1.5 and 2 cm over a length of 4-6 cm. The effects of pulling rate and rotation rate were studied in the range of 2.9-6 cm/hr and 13-70 rpm, respectively. The crystals were cut along the growth axis; the sections were polished (0.06 μm particle size alumina) and chemically etched (1.5 min in 1 part HF, 1 part H_2O_2, and 2.5 parts water, by volume) to reveal impurity heterogeneities which were studied with interference contrast microscopy.

Theory

The theory of interface instability for a two-component system solidfying with planar front under conditions of constitutional supercooling has been developed by a number of investigators. If $\Phi(x, t)$ describes the shape of the perturbed interface, it can be expressed by a Fourier integral (12)

$$\phi(x,t) = \frac{1}{2\pi}\int_{-\infty}^{\infty} e^{i\omega x}\,\Phi_0(\omega)\,e^{tf(\omega)}\,d\omega \qquad [1]$$

and

$$\frac{\dot{\Phi}}{\Phi} \equiv \left(\frac{d\Phi}{dt}\Big/\,\Phi\right) = f(\omega) \qquad [2]$$

where $\Phi_0(\omega)$ is the Fourier transform of the initially perturbed shape of the interface, Φ is the Fourier transform of ϕ, and ω is the spatial frequency associated with the perturbation; $f(\omega)$ is not strongly time dependent, provided the system is just on the verge of instability (12).

A stability criterion can be established based on the values of $f(\omega)$; it can be positive, negative, or complex corresponding to enhancement, decay, or oscillation of a perturbation, respectively. On the basis of this analysis the stability criterion derived for systems with rotational stirring takes the form (15)

* Electrochemical Society Student Member.
** Electrochemical Society Active Member.
[1] Present address: Allied Chemical Company, P.O. Box 1021R, Morristown, New Jersey 07960.
Key words: interface instability, germanium, constitutional supercooling, crystal growth.

$$\frac{K_l G_l + K_s G_s}{(K_l + K_s) G_l} > S\left(-\frac{D}{\nu}\right)^{1/3} 0.75 \quad [3]$$

where K_l and K_s are the thermal conductivities of the liquid and the solid, respectively; G_l and G_s are the thermal gradients near the interface in the liquid and the solid; ν is the kinematic viscosity of the melt; D is the diffusion coefficient of the solute in the melt; and S is the constitutional supercooling parameter defined as

$$S = \frac{C_l - C_s}{\frac{D}{V} G_l} \left| \frac{dT}{dC} \right| \equiv \frac{mG_c}{G_l} = \frac{-m(1-k)VC_o}{G_l D[k + (1-k)\exp - \delta V/D]} \quad [4]$$

where C_l and C_s are the impurity concentrations in the liquid and the solid, respectively, near the interface; V is the instantaneous microscopic growth rate; m is the slope of the liquidus in the phase diagram; k is the equilibrium distribution coefficient; C_o is the impurity concentration in the bulk of the melt; and δ is the thickness of the boundary layer. G_c is the concentration gradient in the liquid just ahead of the advancing interface given by

$$G_c = \frac{-(1-k)VC_o}{D[k + (1-k)\exp -\delta V/D]} \quad [5]$$

Thus, the stability criterion becomes

$$\frac{-m(1-k)VC_o}{D[k + (1-k)e^{-\delta V/D}]} \left| \frac{D}{\nu} \right|^{1/3} 0.75 < \frac{K_l G_l + K_s G_s}{(K_l + K_s)} \quad [6]$$

If the pulling rate V_o, and the impurity concentration, C_o, in the melt are adjusted so that the system is at the verge of instability (*i.e.*, left-hand side of inequality (Eq. [6]) just exceeds the righ-hand side), then during rotational pulling the instantaneous microscopic growth velocity (17), V, is given by

$$V = V_o(1 - \alpha \cos 2\pi Rt) + \frac{d\phi}{dt} \quad [7]$$

where $\alpha = 2\pi R\Delta T/G_l V_o$; ΔT is the temperature variation for a given point at the growth interface over the rotational cycle; and R is the rotational rate. The first term (Eq. [7]) represents the growth rate fluctuations associated with the rotational pulling in a thermally asymmetric system;[2] the second term is the derivative of the perturbation (Eq. [1]) which arises from the instability due to constitutional supercooling. This second term is relatively small and associated with a spatial frequency.

Growth interface shape in time and space.—For a perturbation of constant spatial frequency, by integrating Eq. [1] and employing a delta function, one obtains

$$\phi(x,t) = \frac{1}{2\pi} \Phi_o(\omega) e^{i\omega x} e^{f(\omega)t} \quad [8]$$

If $f(\omega)$ is complex, say, $f(\omega) = p_j(\omega) = Re[p_j(\omega)] + iIm[p_j(\omega)]$, then the shape of the growth interface is given by either the real or imaginary parts of Eq. [9]

$$\phi(x,t) = \Phi_o(\omega) e^{Re[p_j(\omega)]t} \sin\{\omega x + Im[p_j(\omega)]t\} \quad [9]$$

where $\phi_o(\omega) = \Phi_o(\omega)/2\pi$. [The notation adopted here is used by Delves (15).] If the growth rate is constant and the system is on the verge of instability (*i.e.*, inequality, Eq. [6], is just reversed and $Re[p_j(\omega)]$ is small or zero) the general equation representing the one-dimensional growth interface moving in the z direction can be found by integrating Eq. [7] with respect to t

$$z = V_o t + \Phi_o(\omega) \sin\{\omega x + Im[p_j(\omega)]t\} \quad [10]$$

This equation describes the dynamics of the growth interface with oscillatory instabilities of a wavelength $2\pi/\omega$ and phase velocity $Im[p_j(\omega)]/\omega$. On the basis of Delves's theory (15), the onset of oscillatory instability in Ge for the present experimental conditions should be associated with $\lambda = 80$-90 μm and $Im[p_j(\omega)] = 0.5$-1.0 sec^{-1}. If the growth interface, during rotational pulling, advances with periodically varying velocity, V, the general equation representing a one-dimensional growth interface moving in the z direction assumes the form

$$z = V_o t - \frac{\alpha V_o}{2\pi R} \sin 2\pi Rt + \Phi_o(\omega) e^{Re[p_j(\omega)]t} \sin\{\omega x + Im[p_j(\omega)]t\} \quad [11]$$

Results

During crystal pulling by the Czochralski technique the onset of constitutional supercooling in melts with moderately high doping levels can be delayed by seed rotation since boundary layer thickness is decreased. In the absence of constitutional supercooling, the growth interface remains stable and the microscopic growth rate in the z direction varies in a quasisinusoidal mode within each rotational cycle because of unavoidable thermal asymmetry (first term of Eq. [7]). In the presence of pronounced thermal asymmetry, partial remelting takes place during passage of the interface through the hottest region in the system and "remelt" rotational striations are formed which appear as "smooth" parallel lines delineating the shape of the growth interface at the moment of their formation. During crystal pulling from melts doped to very high levels, constitutional supercooling cannot be suppressed by rotation, for any appreciable growth period, and the interface becomes unstable.

Based on the preceding theoretical considerations, constitutional supercooling depends strongly on the microscopic growth rate (Eq. [4]); thus, sinusoidal growth rate variations associated with rotation may bring the system, within each rotation, periodically to the verge of constitutional supercooling; as a result, oscillatory instability can be brought about and be sustained for prolonged periods of growth.

Oscillatory instability.—The behavior discussed above was experimentally observed as seen in Fig. 1, which depicts an outer region of the grown crystals. The rotational striations, normally "smooth" parallel lines, appear here as "wavy" lines, indicating oscillatory instability without interface breakdown. Since the rotational striations are of the remelt type, the observed amplitude of the elevations and depressions is, of course, less than the maximum amplitude encountered during growth. As is seen in Fig. 1, protrusions of the interface into the melt (maxima) on one striation develop (during growth associated with a 360° rotation) into depressions (minima) on the next striation, while the minima develop into maxima.

This behavior might be interpreted as a "stationary" oscillatory instability with the sinusoidal growth rate variations (resulting from seed rotation) being modulated by an oscillatory instability component. However, examination of the instability as observed in Fig. 2-4 indicates that the behavior observed in Fig. 1 is not typical. The growth direction being normal to the striations, these figures show that the maxima on one striation are displaced laterally on the subsequent striation; the extent of such displacement varies depending on the growth conditions. Such lateral displacement of the oscillatory instability is also consistent with the nonperpendicular alignment of the segregation inhomogeneities within successive striations (see, for example, Fig. 2). These periodic segrega-

[2] The effect of sinusoidal temperature fluctuations on the microscopic growth rate has been independently derived by Hurle *et al.* (18).

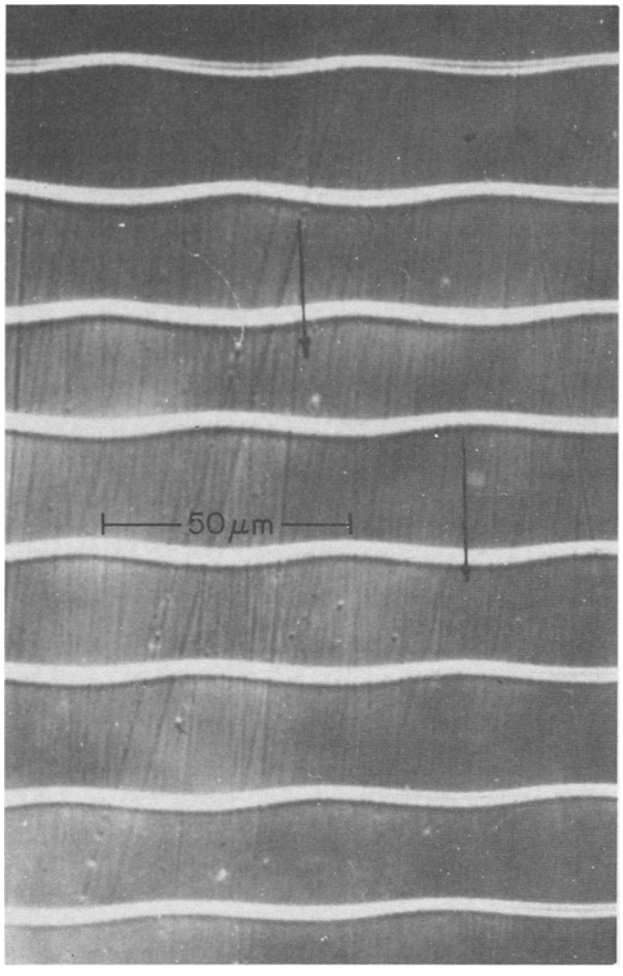

Fig. 1. Rotational remelt striations in a Ga-doped germanium single crystal pulled in the <111> direction (3.15 cm/hr; 26 rpm). The depicted segment is from an outer region of the crystal and shows oscillatory instability of the growth interface. The arrows indicate the direction of growth.

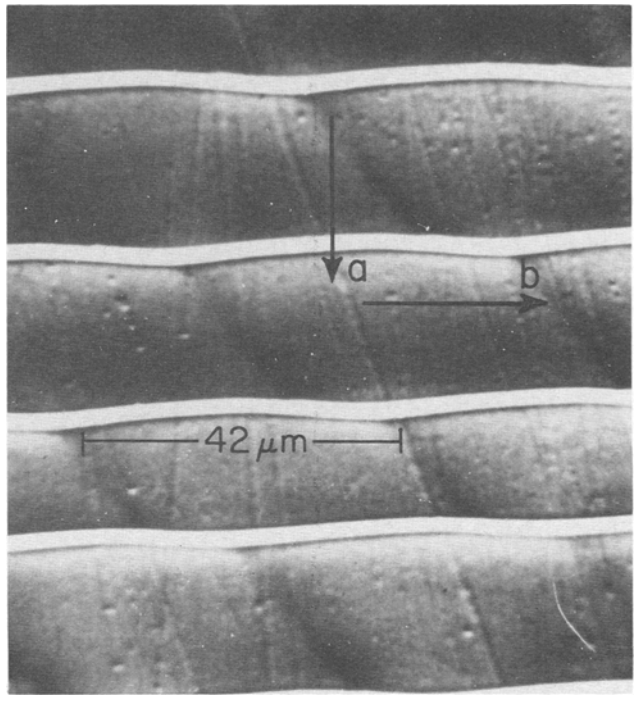

Fig. 2. Oscillatory instability and associated segregation inhomogeneities (inclined dark bands between successive rotational striations). Note lateral displacement of inhomogeneities indicating the traveling wave nature of instability (3.5 cm/hr; 25 rpm). Arrow (a) indicates growth direction and arrow (b) indicates the direction of lateral phase displacement of the oscillation.

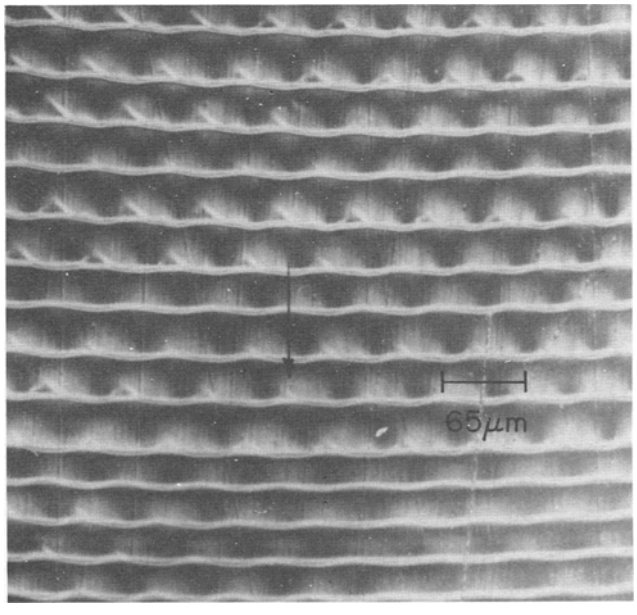

Fig. 3. Effect of rotational rate on interface instability. Depicted segment was pulled at 3.38 cm/hr; the upper and lower regions were rotated at 15 and 20 rpm, respectively (see text).

tion inhomogeneities reflect the periodic development and decay of the instability resulting from the sinusoidal growth rate variations within each rotational cycle. Accordingly, it is concluded that the observed oscillatory instability is of a "traveling wave" nature with a characteristic phase velocity (15) and not stationary as could be assumed from Fig. 1.

Using the cylindrical coordinates system, the oscillatory perturbation can be resolved into two oscillatory components, in the radial and tangential directions, with wavelengths λ_r and λ_θ, respectively. The wavelengths of the oscillations in the radial direction (λ_r) were determined on planes exposed by cutting the crystal along the rotational axis. The wavelengths in the tangential direction (λ_θ) were obtained from cuts perpendicular to the above; since there is an inherent uncertainty in obtaining cuts precisely through the axis of rotation, the measured λ_r and λ_θ values do not necessarily represent the pure radial and tangential components. The phase velocity of the oscillations was determined from the horizontal displacements of the segregation inhomogeneities between successive striations (see Fig. 2) and the rotational rates. It can alternatively be obtained from the displacement of the maxima or minima between successive striations. The values of the experimental data are summarized in Table I.

A direct application of the theory to the present experiments could not be made because not all experimental variables controlling the constitutional supercooling parameter, S, Eq. [4] could be determined. However, since the numerical values assumed in Ref. (15) are sufficiently close to those encountered in the present experiments a comparison between theory and the experimental results is considered reasonable. Thus, the theoretically predicted values of λ_θ given in Table I were obtained from Fig. 3 in Ref. (15), assuming that the fluid velocity in the tangential direction is approximately equal to the macroscopic fluid velocity $2\pi rR$ (19) (a reasonable approximation for the distances from the rotational axis at which λ was measured). It is seen that the experimentally determined values of λ_θ are in reasonable agreement with those predicted from theory for the onset of oscillatory in-

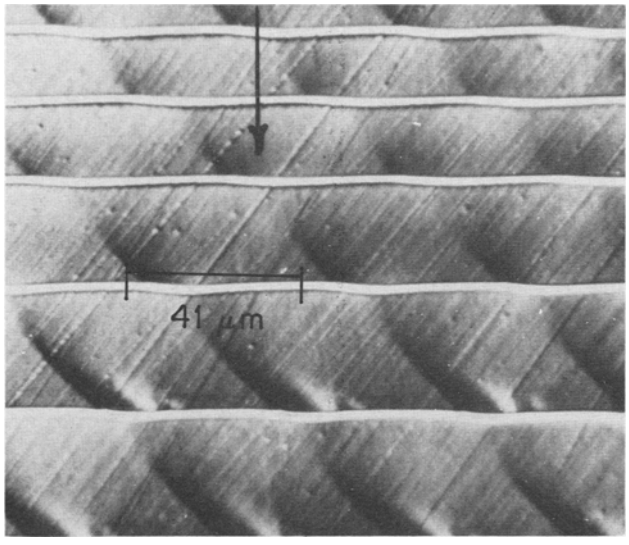

Fig. 4. Effect of pulling rate on interface instability. Depicted segment was rotated at 25 rpm. The upper region was pulled at 2.9 cm/hr (see text).

stability. A similar comparison of λ_r could not be made since a parabolic velocity distribution (assumed in theory) is not applicable for the radial fluid flow.

Effects of pulling rate and seed rotation on oscillatory instability.—The effects of the pulling rate were investigated in crystals grown at fixed seed rotation (25 rpm) with pulling rates ranging from 2.9 to 6.0 cm/hr. The effects of seed rotation were studied in crystals pulled at rates of 2.9 and 3.38 cm/hr with seed rotation ranging from 20-41 and 13-70 rpm, respectively. Since the experimental conditions necessary for the onset of oscillatory instability cannot be arrived at directly from theoretical considerations, the gallium dopant levels were adjusted by trial and error so that the system reached the verge of instability at some time during growth. Amounts of melt several times larger than those corresponding to the size of the crystals pulled were used to insure the occurrence of sustained instability.

The effect of increasing the rate of rotation on the growth process is clearly seen in Fig. 3. Here the depicted upper and lower segments were rotated at 15 and 20 rpm, respectively. While oscillatory instability prevails throughout both segments, the complexity of the segregation inhomogeneities (reflecting the degree of instability) is noticeably reduced in the region grown at the higher rate of rotation. This stabilizing effect reflects a decrease of the average value of the constitutional supercooling parameter, S, due to enhanced stirring. The characteristics of the instability during rotational and nonrotational pulling are compared below.

The effect of the pulling rate on interface instability is shown in Fig. 4. From the spacing of the rotational striations it can be seen that the pulling rate was increased by a factor of about two in the segment of the crystal depicted in the lower part of the figure. This increase in pulling rate clearly resulted in further developed dopant inhomogeneities. It should be noted that the rate of development of the inhomogeneities following each rotational striation is the same in the upper and lower segments of the crystal. The relationship between the observed inhomogeneities and the amplitude of the perturbation is not known in the present case. In view of the pronounced dependence of interface stability on the microscopic growth rate, the behavior observed in Fig. 4 implies that the increase in the pulling rate by a factor of two did not result in a corresponding increase in the microscopic rate of growth during the initial stages of growth following remelting.

Discussion

Theoretical considerations.—The applicability of the interface stability theory to the presently observed oscillatory instability is tested on the basis of typical experimental data employing Eq. [11]. The effects of thermal asymmetry are examined taking $\alpha = 0$ (no thermal asymmetry); $\alpha = 0.9$ (thermal asymmetry, no backmelting); and $\alpha = 1.1$ (backmelting). The growth interface behavior is graphically presented and discussed on the basis of experimental observations. The experimental values employed are: pulling rate, $V_o = 12.5$ μm/sec; rate of rotation, $R = 25$ rpm; distance of instability from rotational axis = 0.6 cm.

When growth takes place in a thermally symmetric environment, $\alpha = 0$, then Eq. [11] reduces to

$$z = 12.5t + 5 \sin\left[\left(\frac{2\pi x}{70}\right) + 1.2t\right] \qquad [12]$$

A graphic representation of Eq. [12] depicting the dynamics of the growth interface, at time intervals of 0.28 sec, is shown in Fig. 5. It is seen that the traveling wave nature of the oscillation (lateral displacement component) modulates the microscopic growth rates thus resulting in periodic regions of decreased and increased growth rates which appear as narrow and wide bands inclined to the advancing growth interface (z direction). The angle of inclination is controlled by the phase velocity of the perturbation. The growth behavior, as shown in Fig. 5, corresponding to

Table I. Wavelengths and phase velocities associated with interface oscillations during Czochralski-type growth of gallium-doped germanium

Crystal number	Rotation rate (rpm)	Pulling rate, V_o (cm/hr)	Initial amount of melt (g)	Radius of the crystal, r_o (cm)	Radial distance of oscillatory instability (cm)	Macroscopic fluid velocity, $V = 2\pi rR$ (cm/sec)	Experimental λ (μm) λ_r	Experimental λ (μm) λ_θ	Theoretical λ_θ (15) (μm)	Experimental phase velocity (μm/sec)
1	25	2.92	312	0.80	0.5 ± 0.1	1.31 ± 0.15	48 ± 3		80	9.6 ± 0.3
2	25	2.93	290	0.75	0.6 ± 0.1	1.51 ± 0.20	49 ± 3		68	10.6 ± 0.3
3	25	3.38	350	0.80	0.7 ± 0.1	1.90 ± 0.20	50 ± 3	65 ± 3	63	14.0 ± 0.4
4	25	3.50	516	0.95	0.5 ± 0.2	1.37 ± 0.15	59 ± 3	70 ± 3	79	11.0 ± 0.5
5*	25	3.50	400	0.95	0.85 ± 0.1	2.36 ± 0.10	41 ± 3	58 ± 3	56	8.9 ± 0.4
6	25	4.50	346	0.75	0.6 ± 0.1	1.51 ± 0.25	62 ± 3	70 ± 3	69	13.9 ± 0.4
7	25	5.50	336	0.75	0.7 ± 0.1	1.76 ± 0.25	64 ± 3		64	13.6 ± 0.4
8	25	5.80	325	0.75	0.6 ± 0.1	1.51 ± 0.25	61 ± 4		69	13.8 ± 0.4
9	20	2.93	310	0.75	0.6 ± 0.1	1.26 ± 0.20	52 ± 3	75 ± 3	85	8.7 ± 0.3
2	25	2.93	290	0.75	0.6 ± 0.1	1.64 ± 0.20	49 ± 3		68	10.6 ± 0.3
10	33	2.93	270	0.75	0.6 ± 0.1	2.10 ± 0.30	40 ± 3		58	11.0 ± 0.3
11	41	2.93	250	0.75	0.6 ± 0.1	2.67 ± 0.30	41 ± 3		55	14.0 ± 0.4
12**	13	3.38	504	0.85	0.6 ± 0.1	0.84 ± 0.15	75 ± 3	82 ± 3	112	13.4 ± 0.6
3	25	3.38	350	0.80	0.7 ± 0.1	1.90 ± 0.20	50 ± 3	65 ± 3	63	14.0 ± 0.4
13	55	3.38	429	0.85	0.6 ± 0.1	3.47 ± 0.35	34 ± 3	45 ± 3	39	15.6 ± 0.4
14	70	3.38	432	0.85	0.6 ± 0.1	4.40 ± 0.50	27 ± 3	40 ± 3	30	22.4 ± 0.5

* Ga concentration in the melt in atoms per cent: C_{l_1} (start), 2.56 ± 0.1; C_{l_2} (end), 3.30 ± 0.12.

** Ga concentration in the melt in atoms per cent: C_{l_1} (start), 1.53; C_{l_2} (end), 1.77 ± 0.01.

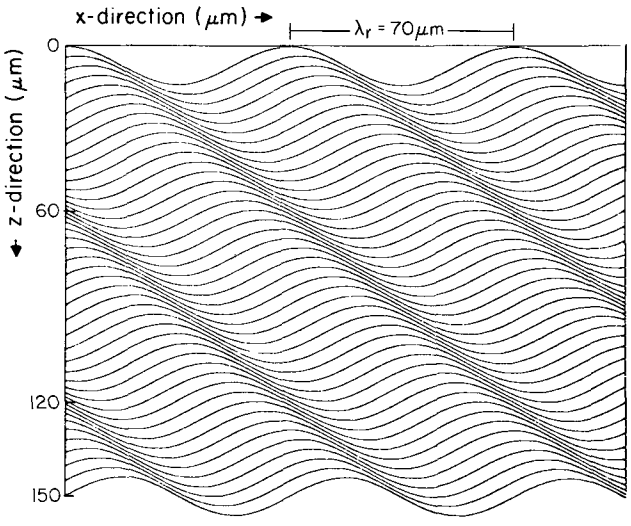

Fig. 5. Graphic presentation of oscillatory growth interface instability (Eq. [12]) in the absence of thermal asymmetry; $\alpha = 0$. The time interval between successive lines is 0.28 sec. (For numerical values used in Eq. [12] see text).

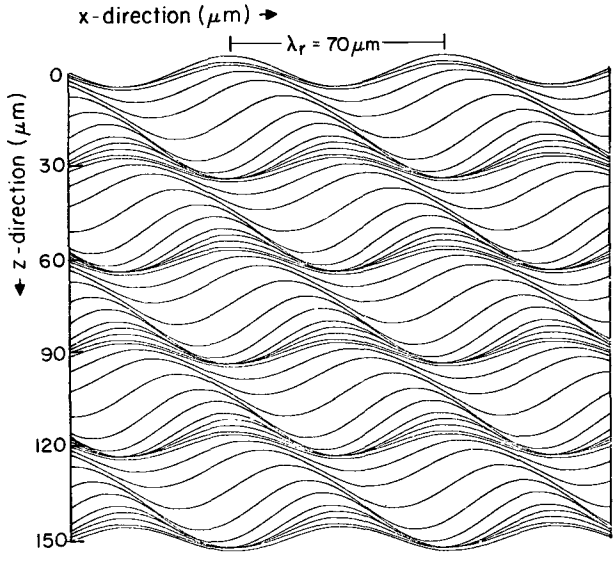

Fig. 6. Graphic presentation of oscillatory growth interface instability in the presence of thermal asymmetry ($\alpha = 0.9$). The interval between successive lines is 0.24 sec (see text).

rotational pulling in the absence of thermal asymmetry, is never encountered in real systems.

In the presence of thermal asymmetry ($\alpha > 0$) the exact solution of Eq. [11] requires the knowledge of the constitutional supercooling parameter (which changes continuously during rotation) since $Re[p_j(\omega)]$ is a function of S.

This behavior is a result of the growth rate dependence of the constitutional supercooling parameter, S; changes in S lead to corresponding changes in $Re[p_j(\omega)]$ between positive and negative values averaging about zero. Depending on whether $Re[p_j(\omega)]$ assumes positive or negative values for extended periods of time, the system will "break down" or revert to stability, respectively. In the presently considered situation characterized by oscillatory instability, the values of $Re[p_j(\omega)]$ remain close to zero. The amplitude of the interface instability, in contrast to that in Fig. 5, is not constant but increases and decreases periodically with the variation of the microscopic growth rate within each rotational cycle. Concurrent with the variation $Re[p_j(\omega)]$, the phase velocity $Im[p_j(\omega)]$ varies periodically; these variations, however, are small. Since S and its variations, during rotation, could not be determined, a graphic representation of a realistic situation ($V_o = 4.5$ cm/hr, $R = 25$ rpm, and $\lambda_r = 70$ μm) was obtained by selecting reasonable values of the phase velocity (ranging from 0 to 30 μm/sec) and amplitude of perturbation (ranging from 4 to 8 μm) for $\alpha = 0.9$ (Fig. 6). The individual lines represent the dynamics of the growth interface morphology at time intervals of 0.24 sec. In this case the microscopic growth rate, dz/dt (which is constant in the absence of thermal asymmetry and oscillatory instability) is modulated simultaneously by: (*i*) the sinusoidal growth rate variation along the z direction (independent of x) resulting from thermal asymmetry and (*ii*) the periodic growth rate variation along both the x and z directions resulting from the traveling wave nature of the oscillatory instability.

When the average value of $Re[p_j(\omega)]$ becomes positive, oscillatory instability can no longer be sustained and the amplitude of the perturbation increases continuously as shown in Fig. 7 and ultimately leads to interface breakdown.

The dynamic behavior of the growth interface under conditions leading to remelting ($\alpha = 1.1$) is presented in Fig. 8. Since in this case the variation of the microscopic growth rate within each rotational cycle is larger than in the case $\alpha = 0.9$, the corresponding variations in phase velocity and amplitude of the perturbation are expected to be larger. Accordingly, the values for the phase velocity were selected to range from 0 to 35 μm/sec and those of the amplitude ranged from 4 to 10 μm. The dotted lines within each rotational cycle represent the grown regions which were remelted during rotation through the hot region of the melt (17). The onset of growth following remelting is indicated in Fig. 8 by heavy lines which correspond to remelt striations (see for example Fig. 2). These

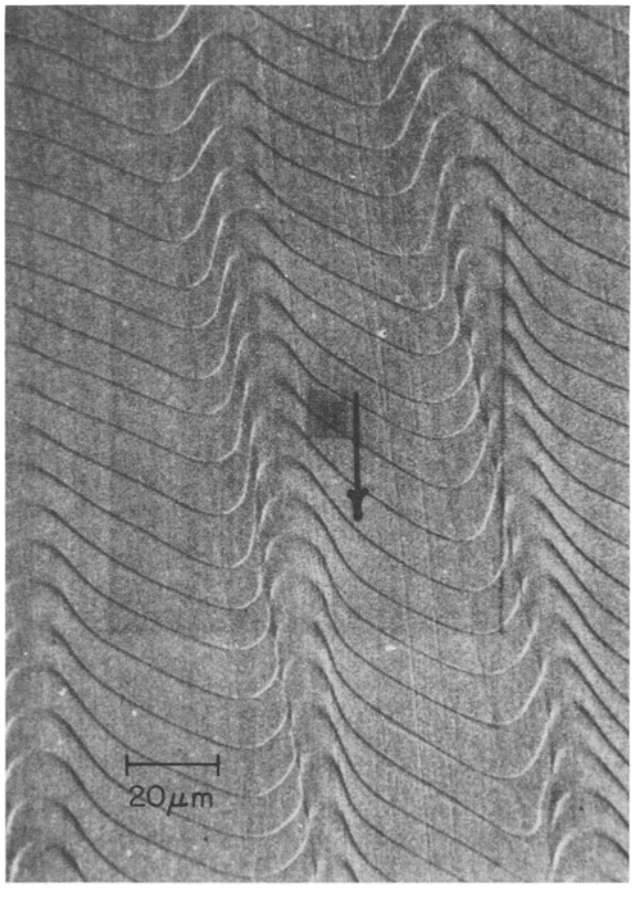

Fig. 7. Interface instability in Ga-doped Ge for growth conditions where the average value of $Re[p_j(\omega)]$ is positive. Oscillatory instability is not sustained; note progressive increase (from top to bottom) of the amplitude of the perturbation.

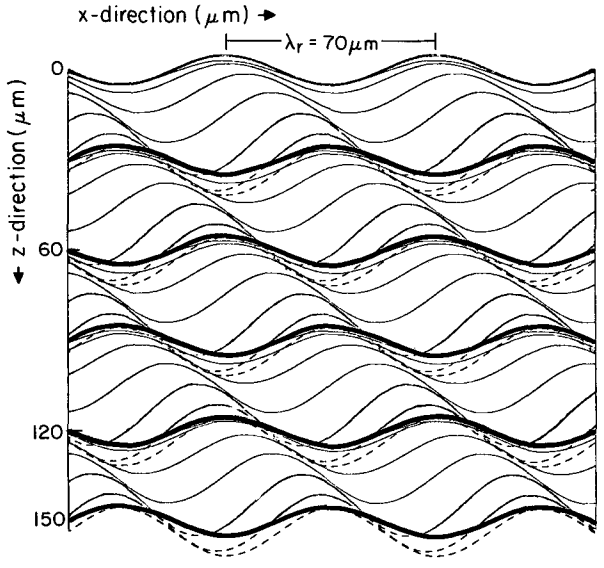

Fig. 8. Graphic presentation of oscillatory growth interface instability under partial remelt conditions ($\alpha > 1$). The dotted lines, within each rotational cycle, represent the grown regions which were remelted. The heavy lines represent the remelt rotational striations. (For comparison with the experimental findings of Fig. 2, see text.)

remelt striations have the wavelength of the oscillatory instability but not its amplitude (the resulting amplitude is significantly reduced).

Comparison with experimental results.—All results in this investigation were obtained on crystals grown in the presence of thermal asymmetry leading to remelting; thus, comparison with theory will be focused on conditions as depicted in Fig. 8. This comparison is based on the premise that the experimentally observed segregation behavior is controlled by the microscopic growth rate.

Consistent with the theoretical considerations outlined above, sustained oscillatory interface instability ("wavy" remelt striations) is observed in all crystals investigated (Fig. 1-4). The traveling wave nature of the oscillation, as predicted from theory, is confirmed by the lateral displacement of the maxima (and the minima) in successive rotational striations, as seen in Fig. 2; the direction of the phase displacement is in agreement with that predicted from theory. The "inclined" segregation inhomogeneities within rotational cycles (between successive rotational striations) seen in Fig. 2 are readily explained on the basis of the preceding analysis; as seen in Fig. 8, the microscopic growth rate, dz/dt, varies along the x direction during each rotational cycle; thus, the traveling wave nature of the oscillations results in the formation of "cells" (between successive remelt striations) bounded laterally by regions of decreased growth rate (inclined bands). The complex segregation inhomogeneities between rotational striations in Fig. 3 cannot be explained exclusively on the basis of growth rate controlled segregation, as discussed below.

Theoretical assumptions and experimental conditions.—The preceding comparison must be viewed in the light of the following basic assumptions underlying the theoretical model (14): (*i*) the growth system is at steady state; (*ii*) the perturbations at the growth interface are small, so that the linearized theory is applicable; (*iii*) fluid flow at the momentum boundary layer is laminar with a parabolic velocity distribution within the boundary layer (diffusion of heat and convective solute transport are dominant); (*iv*) kinetic supercooling is absent; (*v*) there are no radial temperature and concentration gradients.

During rotational crystal growth by the Czochralski technique "steady state" [assumption (*i*)] prevails on a macroscopic level for conditions of constant pulling rate and constant crystal diameter (constant macroscopic growth rate). However, since thermal asymmetry is inherent in Czochralski growth, the microscopic growth rate is not constant but varies periodically within each rotational cycle.

When $\alpha < 1$ the effects of varying microscopic growth rates on interface instability can in principle be quantitatively accounted for through corresponding variations of the constitutional supercooling parameter, S. The growth and segregation behavior under such conditions has been discussed in the previous section. When $\alpha > 1$, as in the presently discussed experiments, partial remelting takes place within each rotational cycle. Since the solute redistribution within the boundary layer associated with the remelt process cannot be assessed, the magnitude of the constitutional supercooling parameter cannot be determined and the applicability of the instability theory cannot be quantitatively tested. The good agreement between theory and experiment in the case of Fig. 2 is attributed to marginal remelt conditions (α very close to 1).

The exact amplitude of the perturbations at the growth interface [assumption (*ii*)] could not be experimentally determined. However, the fact that the oscillatory perturbations were sustained over a considerable period of growth, without leading to interface breakdown, is direct evidence that, even during maximum microscopic growth rate (within each rotation), the amplitude of the perturbation was small enough to keep the system on the verge of instability.

The condition of laminar flow and parabolic velocity distribution in the momentum boundary layer [assumption (*iii*)] was met, in the present system, at the pulling rates (2.0-5.8 cm/hr) and the rotational rates (13-40 rpm) employed. Apparently, under these conditions diffusion of heat and convection controlled solute transport were dominant (15).

The presence of oscillatory instability in all crystals investigated was limited to their outer regions where kinetic supercooling [assumption (*iv*)] approaches zero; oscillatory instability was never encountered in "facet" regions.

Radial temperature and concentration gradients do exist in Czochralski growth; however, their magnitude is small over the regions investigated and can be neglected [assumption (*v*)].

The theoretical treatments of interface instability indicate that crystal rotation during Czochralski pulling has a stabilizing effect through changes in the characteristics of the boundary layer. This conclusion is based on the assumption that rotation takes place in a thermally symmetric environment in which rotation does not affect the microscopic growth rate. Since, however, thermal asymmetry is inherent in Czochralski growth, this assumption is valid only at high rates of rotation since increased stirring tends to minimize thermal asymmetry. At moderate rates of rotation (say, up to 50 rpm) the microscopic growth rate does not remain constant, particularly under remelt conditions where the actual growth rate ranges from negative values (remelting) to positive values which may exceed the pulling rate by more than a factor of ten. It is, thus, clear that in this range of rotational rates, the modulation of the microscopic growth rate can have pronounced destabilizing effects on the growth system. These effects can dominate the concurrent stabilizing effects of stirring. In fact, at moderate rates, seed rotation will induce interface instability rather than have the expected stabilizing effects.

Acknowledgment

The authors are indebted to the National Science Foundation for financial support and to Mr. Clifford J. Herman for his skillful assistance in the growth of the single crystals.

Manuscript submitted June 4, 1973, revised manuscript received Sept. 30, 1973.

Any discussion of this paper will appear in a Discussion Section to be published in the December 1974 JOURNAL. All discussions for the December 1974 Discussion Section should be submitted by Aug. 1, 1974.

REFERENCES

1. J. W. Rutter and B. Chalmers, *Can. J. Phys.*, **31**, 15 (1953).
2. W. A. Tiller, K. A. Jackson, J. W. Rutter, and B. Chalmers, *Acta Met.*, **1**, 428 (1953).
3. D. T. J. Hurle, *Solid-State Electron.*, **3**, 37 (1961); W. Bardsley, J. M. Callan, H. A. Chedzey, and D. T. J. Hurle, *ibid.*, **3**, 142 (1961).
4. W. W. Mullins and R. F. Sekerka, *J. Appl. Phys.*, **35**, 44 (1964).
5. V. V. Voronkov, *Soviet Phys.-Solid State*, **6**, 2378 (1965).
6. R. F. Sekerka, *J. Appl. Phys.*, **36**, 264 (1965).
7. R. T. Delves, *Phys. Status Solidi*, **16**, 621 (1966); *ibid.*, **17**, 119 (1966).
8. R. F. Sekerka, in "Crystal Growth," H. S. Peiser, Editor, p. 691, Pergamon Press, Oxford, England (1967).
9. S. R. Coriell and R. L. Parker, *ibid.*, p. 703.
10. L. A. Tarshis and W. A. Tiller, *ibid.*, p. 709.
11. G. R. Kotler and W. A. Tiller, *ibid.*, p. 721.
12. R. F. Sekerka, *J. Crystal Growth*, **3, 4**, 71 (1968).
13. D. T. J. Hurle, *ibid.*, **5**, 162 (1969).
14. R. T. Delves, *ibid.*, **3, 4**, 562 (1968).
15. R. T. Delves, *ibid.*, **8**, 13 (1971).
16. R. Singh, A. F. Witt, and H. C. Gatos, *J. Appl. Phys.*, **41**, 2730 (1970).
17. K. Morizane, A. F. Witt, and H. C. Gatos, *This Journal*, **113**, 51 (1966); *ibid.*, **114**, 738 (1967); *ibid.*, **115**, 747 (1968).
18. D. T. J. Hurle, E. Jakeman, and E. R. Pike, *J. Crystal Growth*, **3, 4**, 633 (1968).
19. Y. G. Levich, "Physicochemical Hydrodynamics," Prentice-Hall, Inc., Englewood Cliffs, N. J. (1962).

A Diffusion Model for Oxidation of Nickel-Iron Alloys at 1000°C

A. D. Dalvi*,[1] and W. W. Smeltzer*

Department of Metallurgy and Materials Science, McMaster University, Hamilton, Ontario, Canada

ABSTRACT

A generalized diffusion model involving ternary oxides is used to formulate the oxidation mechanism of Ni-Fe alloys containing 2 and 4 weight per cent Fe. A defect structure, adopted for the inner nickel oxide layer containing iron, yields the variation of its cation diffusion coefficients which, when substituted in the diffusion equations, yield the cation concentration and the oxygen activity profiles in the oxide and the oxidation constants for the respective alloy. Thermodynamic considerations are used in deriving the oxygen activity profile in the outer two-phase nickel oxide-spinel layer of an external scale. A solution to the diffusion problem in the alloy is considered. The experimentally derived composition path in an alloy and the scale is superimposed on the Fe-Ni-O phase diagram. This path is shown to be consistent with the structural observations and composition determinations, and it is also consistent with thermodynamic and kinetic considerations.

In an earlier work (1) the present authors discussed the kinetics and morphological development of the oxide scales formed at 1000°C on Ni-Fe alloys containing 0-25 weight per cent (w/o) Fe. It was demonstrated that continuous and reproducible long-time kinetic curves could be obtained in dry oxygen. Since the over-all reaction kinetics and growth of individual layers followed a parabolic time dependence, it is reasonable to assume that conditions of ambipolar diffusion and local equilibrium at interfaces would occur at this high temperature. Accordingly one may postulate a mechanism based on diffusion through the different phases. The purpose of this paper is to present experimental results for the iron and nickel distributions in the various phases present during the oxidation of these alloys and to rationalize the oxidation kinetics for these alloys on the basis of a ternary diffusion model.

Experimental Procedures and Results

The alloys oxidized contained 0-25 w/o Fe. The samples, which were in the form of 1 × 2 × 0.1 cm plates, were sectioned after oxidation and mounted and polished for metallographic examination and electron-probe microanalyses. Oxidation was carried out at 1000°C in pure oxygen contained in a volumetric apparatus at 400 Torr pressure. Details of the experimental procedures are given in Ref. (1). The nominal and actual compositions of the alloys of interest here are reproduced in Table I.

Concentration profiles of nickel and iron across the samples were determined from samples oxidized for various periods up to 55 hr. The instrument used was a CAMECA MS-24 Model electron microprobe. Counts on Ni and Fe K_α x-rays were taken at regular intervals across the samples and the concentrations were obtained using the pure metals as standards and a procedure described in Ref. (2).

Table I. Compositions of the investigated alloys based upon wet chemical analyses for nickel and iron

Nominal composition	Actual composition	
	w/o Fe	w/o Ni
Ni-2% Fe	1.85	98.15
Ni-4% Fe	4.5	95.5
Ni-6% Fe	6.6	95.4
Ni-8% Fe	8.3	91.7

* Electrochemical Society Active Member.
[1] Present address: J. Roy Gordon Research Laboratory, The International Nickel Company of Canada Limited, Mississauga, Ontario, Canada.

Key words: Ni-Fe alloys, NiO, $(Ni,Fe)_3O_4$, alloy oxidation, diffusion model.